Dynamic Response Analysis of Slab Subjected to Central Contact Blast: Exploring Effects of Blast Placement on Compression and Tension Faces

S. M. Anas[1*], *Mohd* Shariq[1], *Mehtab* Alam[2], *Narhol* Eshkaraeva[3], *Karomat* Matyaqubova[4]

[1]Department of Civil Engineering, Jamia Millia Islamia (A Central University), 110025 New Delhi, India
[2]Department of Civil Engineering, Netaji Subhas University of Technology, 110073 New Delhi, India
[3]Department of Applied Mathematics, Karshi State University, 180117 Karshi, Uzbekistan
[4]Urgench State University, Urgench 220100, Uzbekistan

Abstract. The fortification of military and civilian infrastructures against explosive events has garnered heightened consideration among structural engineers, owing to the surge in subversive detonations and inadvertent blasts witnessed in recent times. Notable examples include the Beirut port explosion in 2020 and the Kabul airport attack in 2021, which underscore the critical need for enhanced protective measures in structural design. In the domain of structural engineering, safeguarding slender structural elements, notably slabs, emerges as a pivotal concern. Slabs, integral constituents within architectural constructs, bear significant responsibility in upholding structural integrity and providing support. Nonetheless, their slender configuration exposes them to heightened vulnerability in the face of detonations, particularly those initiated by direct contact. In contrast to sturdier structural components like columns or walls, slabs exhibit diminished mass and intrinsic resilience, rendering them predisposed to deformation, fracturing, and ultimate failure when subjected to explosive forces. This research employs an Integrated Eulerian Lagrangian formulation within the framework of the FEM, utilizing the dynamic computational tool Abaqus/Explicit. Its objective is to scrutinize the behavior and efficacy of a mono-reinforced one-way concrete slab when subjected to a central contact explosion. The computational model undergoes validation through comparison with experimental findings readily available in the public domain. Subsequently, the validated model is applied to explore the response of the slab in two distinct scenarios: in the initial configuration, the TNT charge is positioned on the upper surface, designated as the compression face, while in an alternate configuration, it is situated on the lower surface, known as the tension face. The damages incurred by the slab for the two distinct blast scenarios are compared to gain better insight into the structural response under differing blast conditions. Results showed that the placement of TNT explosives at the lower surface (tension face) of the slab (Scenario: II) led to increased upward deformation and tensile stress in reinforcement bars compared to Scenario I. Specifically, Scenario II exhibited a 1.27-fold increase in deformation and heightened stress intensity, indicating greater severity in terms of damage and structural failure potential.

1. Introduction

Recently, there has been a notable surge in the attention directed towards explosive loads, primarily prompted by a myriad of inadvertent or deliberate occurrences that have adversely impacted critical structures worldwide, endangering their inhabitants [1-2]. Conventional structures, typically devoid of specific design considerations to withstand blast loads, find themselves vulnerable to such events [3]. Given that the designated load magnitudes in conventional structural design are notably dwarfed by those generated in most explosive scenarios, these structures become susceptible to significant damage upon exposure to such assaults. Consequently, the architectural landscape has witnessed a burgeoning emphasis on the structural fortification against shock and blast wave impacts. Explosive threats possess the capability of being triggered in close proximity to their intended targets, culminating in the propagation of high-pressure waves and airborne debris capable of inflicting substantial harm upon individuals and edifices alike [1]. Recent examples of such events include: (i) the devastating explosion in the port of Beirut, Lebanon, in August 2020,

*Corresponding author: mohdanas43@gmail.com

resulting from the detonation of improperly stored ammonium nitrate, which caused extensive damage to surrounding buildings and claimed numerous lives; (ii) the explosion at a chemical plant in the city of Leverkusen, Germany, in July 2021, triggered by a fire, which released toxic gases and caused significant structural damage, leading to casualties and extensive environmental repercussions; (iii) the explosion at a fertilizer plant in the town of Dzerzhinsk, Russia, in June 2022, resulting from a fire and subsequent detonation of stored ammonium nitrate, causing widespread destruction and environmental contamination; (iv) The blast at a military base in Bata, Equatorial Guinea, in March 2023, caused by the accidental detonation of munitions, resulting in a large number of fatalities, injuries, and extensive damage to nearby residential areas; and (v) The explosion at a chemical facility in Tianjin, China, in December 2023, triggered by the mishandling of hazardous materials, leading to a massive blast that devastated the surrounding area, claiming numerous lives and causing extensive damage to property.

Therefore, a comprehensive comprehension of the mechanics underlying an explosion is imperative prior to the acquisition and meticulous analysis of explosion-related data, as well as the anticipation of impact characteristics. A detonation signifies the abrupt liberation of energy resulting from a chemical reaction on a substantial scale. This surge in energy elevates the ambient air temperature to approximately 3000 degrees Celsius, engendering high-pressure gas shock waves that emanate with initial pressures of approximately 3 x 10^7 Pascals at the point of origin. These waves propagate from the epicenter of the explosion at velocities nearing 7000 meters per second. The phenomenon of a blast transpires over an exceedingly brief interval, typically within milliseconds. In the case of an explosive device situated at ground level, the pressure wave instantaneously rebounds and amplifies upon encountering the ground surface, subsequently dispersing from the source in the configuration of a hemispherical wave front if unimpeded by obstacles. Upon collision with a structure, the blast wave undergoes reflection and augmentation in accordance with the angle of incidence relative to the structure's surface type. The magnitude of peak overpressure, which denotes the pressure exceeding standard atmospheric pressure, and the duration of such overpressure, fluctuate contingent upon the distance from the explosive device. Furthermore, these parameters' values are influenced by the composition of the explosive materials constituting the bomb; typically, the bomb's size is quantified in terms of an equivalent weight in Trinitrotoluene (TNT).

The behavior of concrete infrastructures and components to the force of explosive impact is contingent upon several factors, including the properties of the blast itself, the intricate interplay of geometric and dynamic structural features, as well as the material's distinctive dynamic response attributes [3].

The strategic targeting of slabs with explosives for contact blasts represents a particularly straightforward method of subversion, especially when contrasted with alternative approaches within structural demolition. Notably, slabs constitute integral components of buildings, serving as essential elements for structural integrity. As thin flexural members, slabs play a pivotal role in distributing loads and providing support throughout the edifice. However, their inherent thinness renders them especially susceptible to the destructive forces unleashed by explosions. Consequently, contact blasts upon slabs often yield more significant damage compared to close-in blasts. This destructive potential is evidenced by localized manifestations such as concrete cratering, scabbing, and the disruption of reinforcement mechanisms.

The delay in experimental research assessing the blast resistance capabilities of building components arises from various factors, including limited access to testing facilities, exorbitant transportation expenses for transporting specimens to testing sites, rental fees for specialized equipment necessary for conducting studies and trials, and the inherent dangers associated with live explosion testing. These impediments curtail both the quantity of tests feasible and the range of parameters that can be explored in each testing regimen. Conversely, recent advancements in computer software and hardware offer a viable alternative: numerical modeling. This method facilitates comprehensive inquiries into various design aspects and factors at a significantly reduced cost compared to traditional physical testing methods.

2. Investigative Objectives and Research Novelty

A sophisticated Finite Element Method (FEM) software suite, Abaqus, renowned for its high-fidelity simulations, is employed to meticulously analyze and predict the repercussions of contact blast on a slab. This slab typically incorporates HRB335 bars, each boasting a diameter of 6mm, spaced at intervals of 75mm center-to-center (denoted as "c/c"). The precision and reliability of the numerical model are corroborated through rigorous validation against experimental findings [4] documented in the public domain.

The primary aim of this research endeavor is to explore the impact of concentric contact explosion on the dynamic characteristics of a unilaterally supported slab. This investigation extends to two distinct scenarios: in the initial case, the TNT charge is situated at the upper surface, known as the compression face, while in the alternate case, it is positioned at the lower surface, referred to as the tension face. The novelty of this investigation lies in its endeavor to assess the severity of structural damage resulting from two distinct blast scenarios. Notably, the current literature predominantly focuses on explosive placement atop the slab's upper face. However, there exists a discernible gap in understanding the slab's response when the explosive charge is positioned at the lower face. Given the practical feasibility of both scenarios, it is imperative to delve into this unexplored territory and comprehensively investigate the dynamic responses under such conditions.

3. Concise Literature Review

Numerous scholars [4-12] have depended on combining a restricted set of experimental trials with computational simulations to analyze how structural components react to explosive loading, owing to the notably greater expenses linked with conducting live explosion tests.

Zhao et al. [13] conducted a computational investigation into the dynamic response of innovative reinforced concrete (NRC) and traditional reinforced concrete (ORC) slabs subjected to the explosion. The dimensions of the slabs under examination were standardized at 1200mm x 1200mm x 40mm. The research results unveiled that when directly juxtaposed with the ORC slab, the NRC slab, characterized by a reinforcement configuration oriented at a 60-degree angle, exhibited reduced deflections and enhanced resilience against blast-induced forces. Qu et al. [14] conducted a study aimed at elucidating the dynamic characteristics of reinforced concrete (RC) beams with initial cracks subjected to air blast loading. Their findings revealed a notable augmentation in the maximum deflection of the midspan for pre-cracked RC beams when subjected to blast loading. Wang et al. [15] delved into the resilience against blast loading of a RC slab through close-in blast tests, delineating two pivotal thresholds of damage. Zhang et al. [16] observed that diminishing scaled distances correlated with an enlarged spalling region in RC beams exposed to blast loading conditions. Yao et al. [17] undertook a comprehensive exploration, combining numerical simulations and experimental assessments, investigating the blast resistance of RC slabs measuring 850mm x 750mm x 30mm with varying reinforcement ratios. They derived an empirical equation elucidating the correlation between deflection and thickness ratio. Zhao et al. [18] employed a fluid-solid coupling algorithm to scrutinize the mechanisms governing damage and dynamic responses in RC containment structures subjected to internal detonation loading. Li and Hao [8] executed a computational analysis to replicate spall damage experienced by reinforced concrete (RC) columns under blast loading conditions. Their investigation encompassed an examination of the dimensions of the columns as well as the reinforcement ratio, elucidating their effects on the structural response. In a separate study, Castedo et al. [6] explored the behavior of a one-way slab measuring 4400mm x 1460mm x 150mm, which was doubly reinforced with 12mm diameter bars spaced at intervals of 150mm center-to-center. To validate the accuracy of their finite element simulation, the researchers compared their numerical results with field tests conducted on a full-scale blast-loaded slab. Furthermore, Silva and Lu [12] investigated a methodology to assess the influence of charge weight and distance of detonation on the extent of damage sustained by slabs. Their study aimed to provide insights into the parameters governing the structural response to explosive loading, thereby contributing to the understanding of blast-induced damage mechanisms.

Various numerical methodologies, including empirical, ConWEP (empirical-based), Smooth Particle Hydrodynamics (a technique independent of mesh constraints), and Integrated Eulerian Lagrangian (IEL, a method melding the Eulerian and Lagrangian paradigms for dynamic simulations), are employed for simulating the impact of blasts on structures. Past research by [2] demonstrates that the IEL method is regarded as the pinnacle of sophistication and realism in blast modeling techniques.

4. Configuration and Setup of Models

The Integrated Eulerian Lagrangian Finite Element Method (IEL-FEM) within the Abaqus software suite stands as a potent tool for simulating blast events [2-3]. This method integrates the Eulerian approach, proficient in accommodating substantial deformation and high strain rate characteristics of explosive materials, with the Lagrangian method, which excels in portraying the structural response of surrounding materials [19-20]. By means of this amalgamation, the nuanced interaction between the blast wave and the structure can be faithfully reproduced. This approach entails surrounding the structure with an Eulerian domain, which encompasses a volume of air. A dynamic pressure wave is then imposed as a boundary condition within this air domain and subsequently propagated into the structure, represented in the Lagrangian domain [21]. Furthermore, the software facilitates the attainment of desired angles of incidence through the integration of Lagrangian dynamics within the Eulerian computational framework.

In this investigation, the blast phenomenon is simulated utilizing the IEL approach. The three-dimensional computational model, delineated in Figure 1, encompasses the slab, TNT, and ambient atmosphere within a cuboidal domain. The slab is represented by a Lagrange mesh, while the ambient atmosphere and TNT are characterized by an Euler mesh framework. This Eulerian mesh configuration imposes pressure boundaries onto the Lagrange mesh, thereby instigating displacement within the slab. Conversely, the Lagrange mesh imposes a velocity constraint on the Euler mesh, thereby anchoring it in position to prevent interference with the Lagrange mesh. To enhance the fidelity of the simulation, an air region is incorporated into the model. The minimum element length of the air mesh is determined in accordance with [22]. All perimeters of the Eulerian domain are rendered immobile to prevent material escape, while a non-reflective Eulerian boundary is established along the lateral confines of the domain to mitigate the reverberation of pressure waves, thus augmenting the accuracy of simulation results [19-20, 22]. As depicted in Figure 1, a rigid substrate is integrated at the base of the domain to emulate the reverberation of blast shockwaves upon impact with the ground [22]. The pressure within the airspace correlates directly with the atmospheric pressure. Furthermore, clamped boundary conditions are enforced on the opposing edges of the slab.

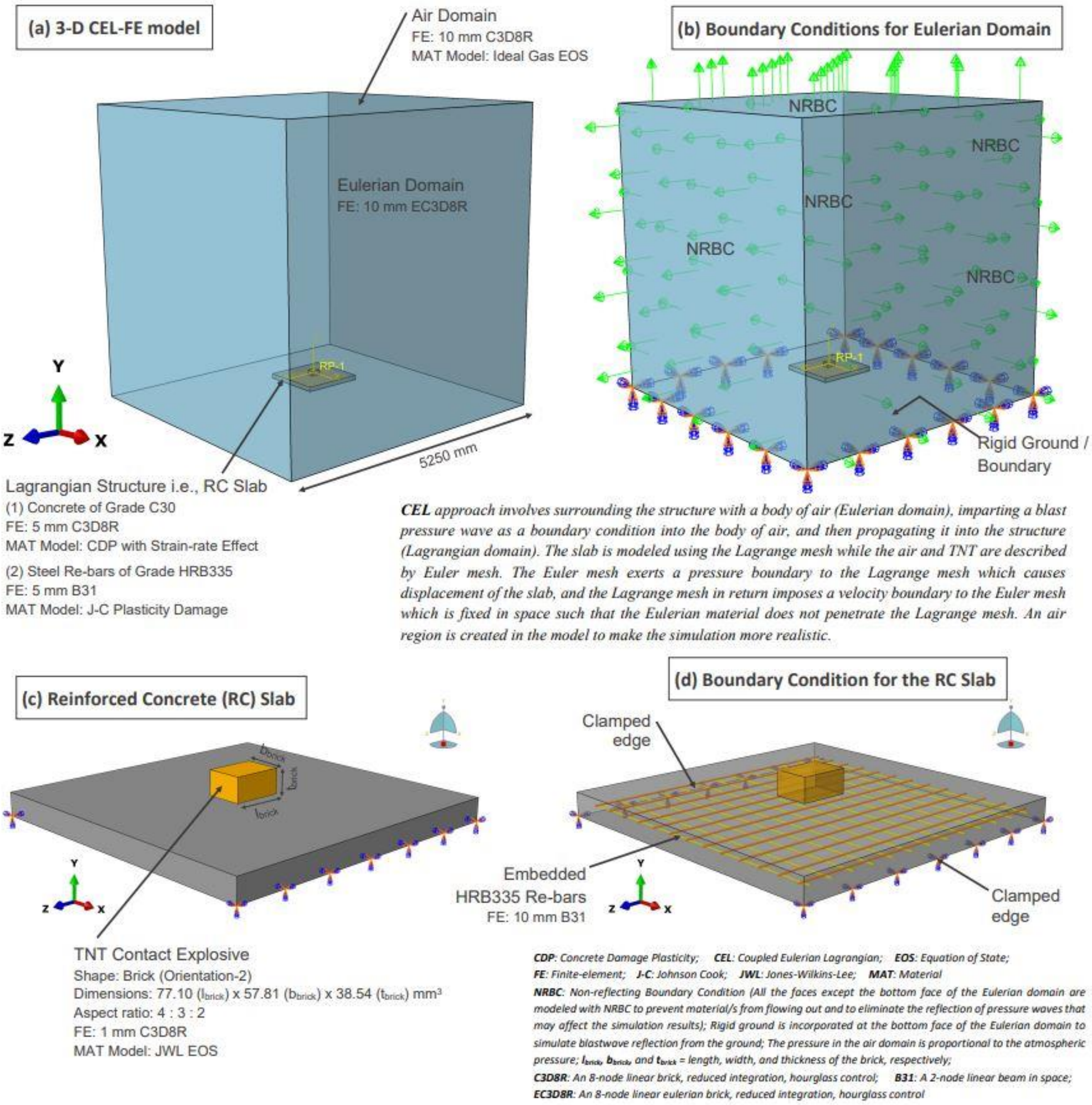

Fig. 1. Configured model for computational explosion analysis using IEL-FEM.

A quantity of TNT weighing 0.28 kilograms, configured in a brick-shaped geometry, was positioned atop the centroid of the slab in accordance with the experimental framework referenced [4]. This same configuration has been adopted for the current numerical analysis. The selection of element type and mesh granularity exerts considerable influence on the desired precision of FE outcomes and computational efficiency. Furthermore, the selected components must conform to the material model utilized in the finite element analysis to guarantee the necessary precision. The explicit C3D8R element type is opted for modeling the concrete component, whereas the B31 element, also falling under the explicit category, is chosen for representing the reinforcement bars [23-25]. The air and explosive materials are discretized employing the C3D8R element type as well. The depiction of reinforcement specifics and slab dimensions is elucidated in Figure 2.

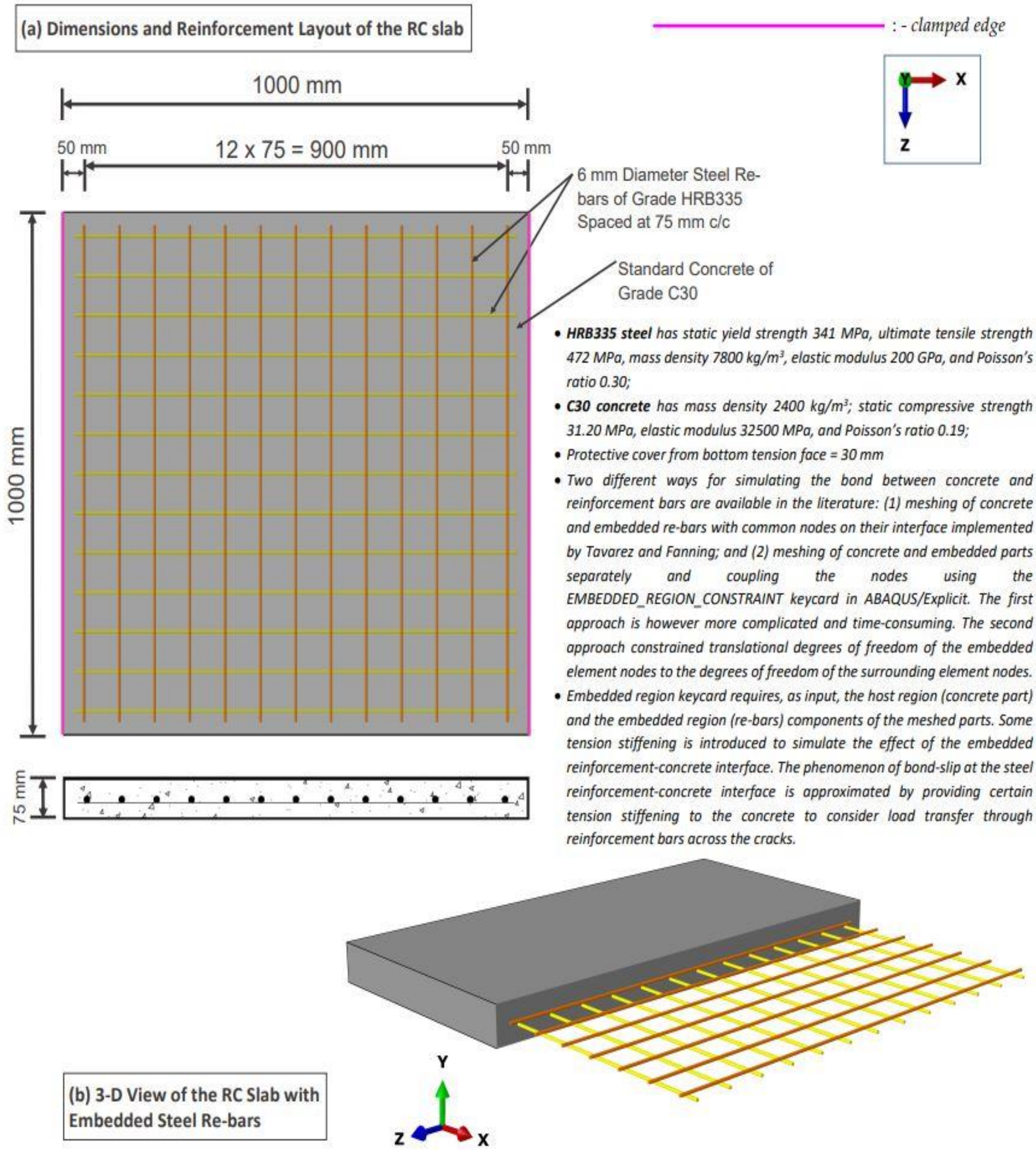

Fig. 2. Codified representation of reinforcement details and slab dimensions.

The reference studies [19-20, 22] extensively elucidate the modeling intricacies of materials such as concrete and steel. It delves into a comprehensive discussion on how strain-rate effects are integrated into the materials models, employing dynamic increase coefficients for this purpose.

The explosive substance, TNT, is delineated through the application of the Jones-Wilkins-Lee EOS, while the atmospheric properties are modeled using the Ideal Gas EOS. Detailed elucidation of these equations of state can be found within the Abaqus manual. The specific properties pertaining to TNT and air are tabulated in the reference studies [19-20, 22], and their inclusion here is omitted to avoid redundancy of data.

Figure 3 depicts the two slabs under investigation in this study, representing distinct scenarios of central contact blast. In Scenario I, the explosive charge of TNT is situated atop the surface, identified as the compression face. Conversely, in Scenario II, the charge is positioned beneath the surface, denoted as the tension face.

 https://doi.org/10.1051/e3sconf/202456302021

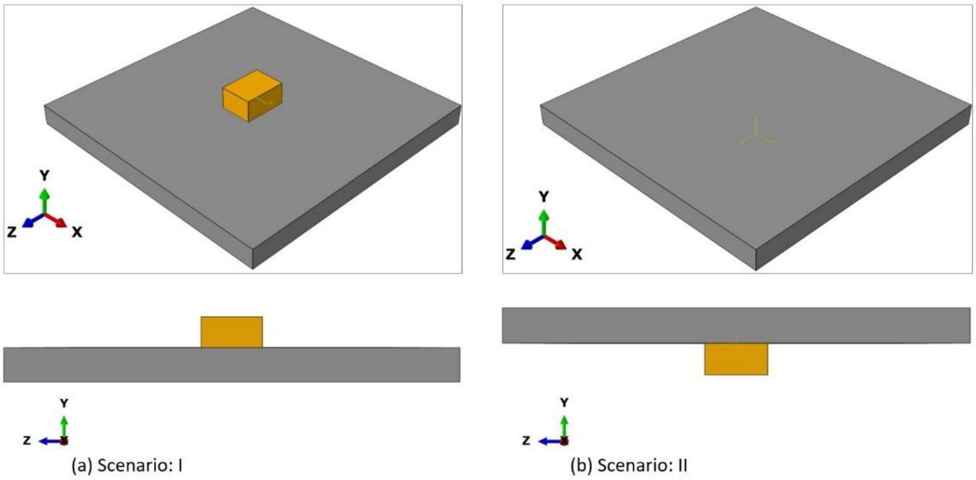

Fig. 3. The slabs examined in this study.

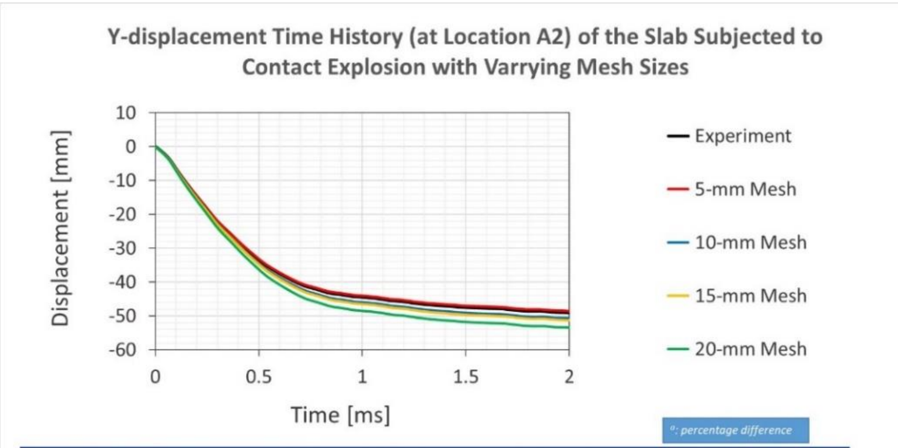

Finite Element Size [mm]	Total Elements	Total Nodes	Maximum Displacement [mm] of the Slab	Computational Time [x 10^4 ms]	Disk Space [GB] used
5	290178029	317687244	-48.55 (^{a}0.92%)	2640	11.84
10	289658029	315055537	-50.76 (3.52%)	1440	8.68
15	289600474	312423075	-51.34 (4.66%)	840	7.98
20	289588029	310918447	-53.57 (8.90%)	720	7.68
Experiment	---	---	-49.0	---	---

Fig. 4. Verification: I.

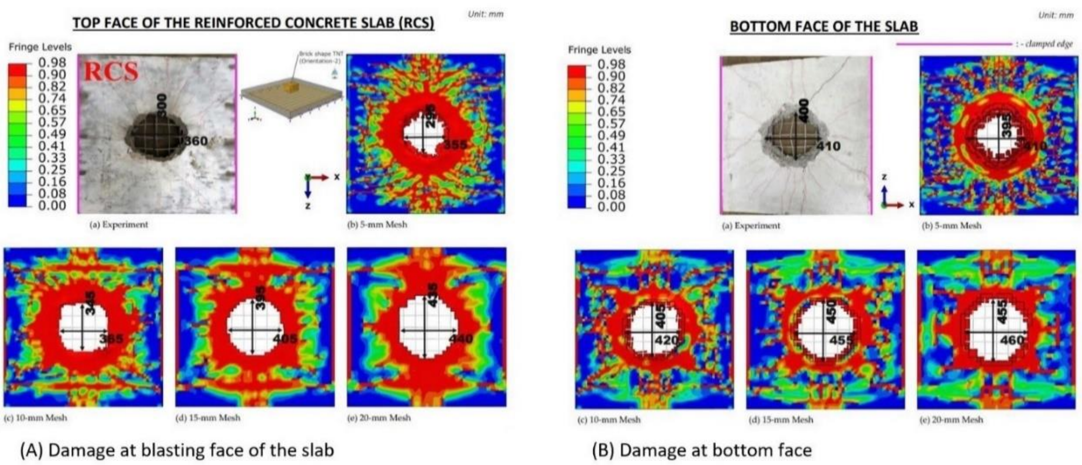

Fig. 5. Verification: II.

5. Verification of the Computational Model

The mesh sensitivity analysis is conducted across varying sizes, specifically 5, 10, 15, and 20mm. Observations indicate a correlation between mesh size and the maximum central vertical displacement, as depicted in Figure 4. Notably, a reduction in mesh size corresponds to a decrease in the maximum central displacement (-Y direction). For instance, utilizing a 5mm mesh size yields a maximum central displacement of 48.55mm, representing a marginal deviation of 0.92% from experimental data. On the contrary, utilization of a 20mm mesh size yields a pronounced deformation of 53.57mm, implying a substantial escalation in deformation of about 9.32% in contrast to empirical observations. Intermediate magnitudes of deformation are discerned for mesh sizes of 10mm and 15mm, yielding peak deformations of 50.76mm (roughly 3.59% above empirical measurements) and 51.34mm (about 4.77% surpassing empirical measurements), respectively. Henceforth, the mesh size of 5mm is deemed appropriate, as it closely emulates the response of the slab under blast conditions, demonstrating a minimal deviation of merely 0.92%. Figure 5 illustrates that damages to the slab, such as cracks and perforation magnitudes, align closely with those documented in the referenced literature [4]. To uphold precision in outcomes, the present study underscores the necessity of utilizing a 5mm element size.

6. Findings and Analysis

Figure 6 to Figure 8, In Scenario: I, the contact blast imposes formidable forces upon the concrete, leading to its pulverization and the subsequent perforation of the slab. The blast inflicts damage by subjecting the affected slab's contact area to shear forces. Moreover, the reinforcement bars undergo substantial deformation, as depicted in Figure 5. The concrete undergoes local bending and shearing, culminating in the manifestation of bending and shearing within the bars. The region directly beneath the explosion experiences significant deformation in the bars. Diverse types of damage afflict the slab, including conspicuous cracks on its upper and lower surfaces, deformations caused by bending or flexure-shear, concrete spalling, and punctures. The reflection of the dynamic wave upon encountering the bottom surface of the slab induces tensile stress on its lower aspect and compressive stress on the upper aspect, precipitating the emergence of cracks on either side. Within the region affected by the blast impact, the concrete succumbs to crushing owing to its reduced ability to endure both compressive and tensile forces, consequently leading to perforation. Remarkably, the underside of the slab manifests a greater concentration of fractures in contrast to the side exposed to the explosion, with the heightened occurrence and depth of cracks on the tension-enduring facet attributed to the insufficient tensile resilience of the concrete.

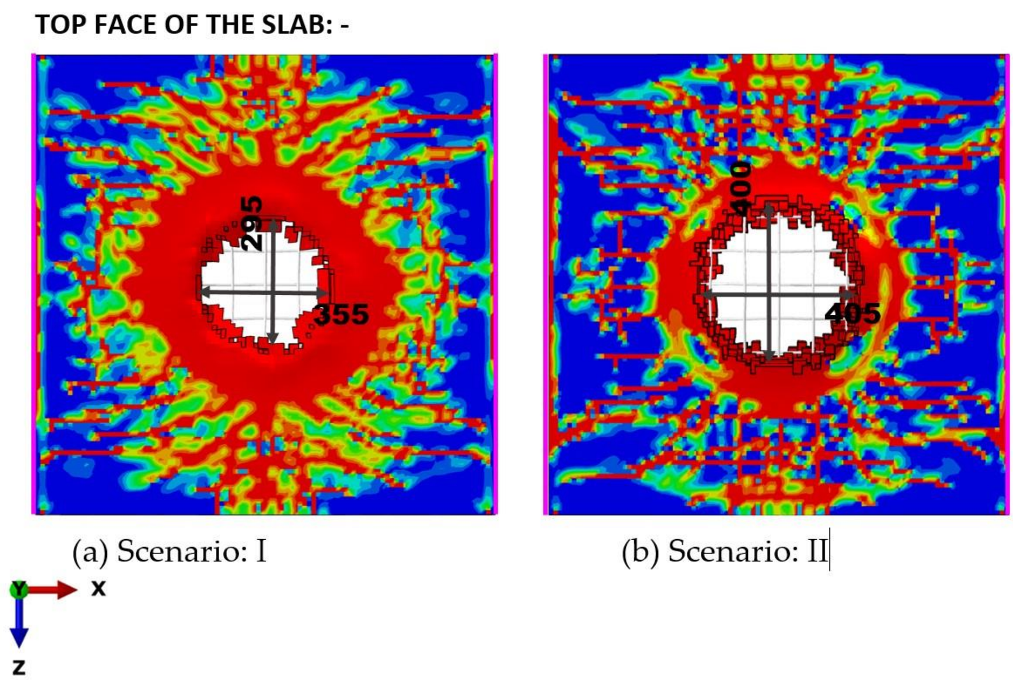

Fig. 6. Damage incurred on the slabs: upper surface.

In Scenario: II, the placement of TNT at the tension face (lower face) of the slab introduces a reverse phenomenon compared to Scenario: I. Here, the contact blast exerts its force primarily upward, causing the slab to experience compression at the lower face and tension at the upper face. Consequently, the response of the slab and its reinforcement

 https://doi.org/10.1051/e3sconf/202456302021

bars is expected to differ from that observed in Scenario: I. Consequently, the structural response is expected to exhibit heightened severity in terms of damage, deformation, and structural failure compared to Scenario: I.

In the context of Scenario: I, the reinforcement bars situated beneath the impacted region exhibit a pronounced downward deformation, reaching a maximum displacement of 48.55mm, Figure 9. Conversely, under Scenario: II conditions, the anticipated maximum upward deformation ascends to 61.92mm, representing a 1.27-fold increase compared to Scenario: I.

Tensile stress has manifested within the reinforcement bars situated beneath the impacted zones of the slabs. In Scenario I, the peak magnitude measures 812.31 megapascals (MPa), whereas in Scenario II, it escalates to 909.56 MPa. Evidently, the severity of Scenario II surpasses that of Scenario I, delineating a discernible discrepancy in stress intensities between the two scenarios, Figure 10.

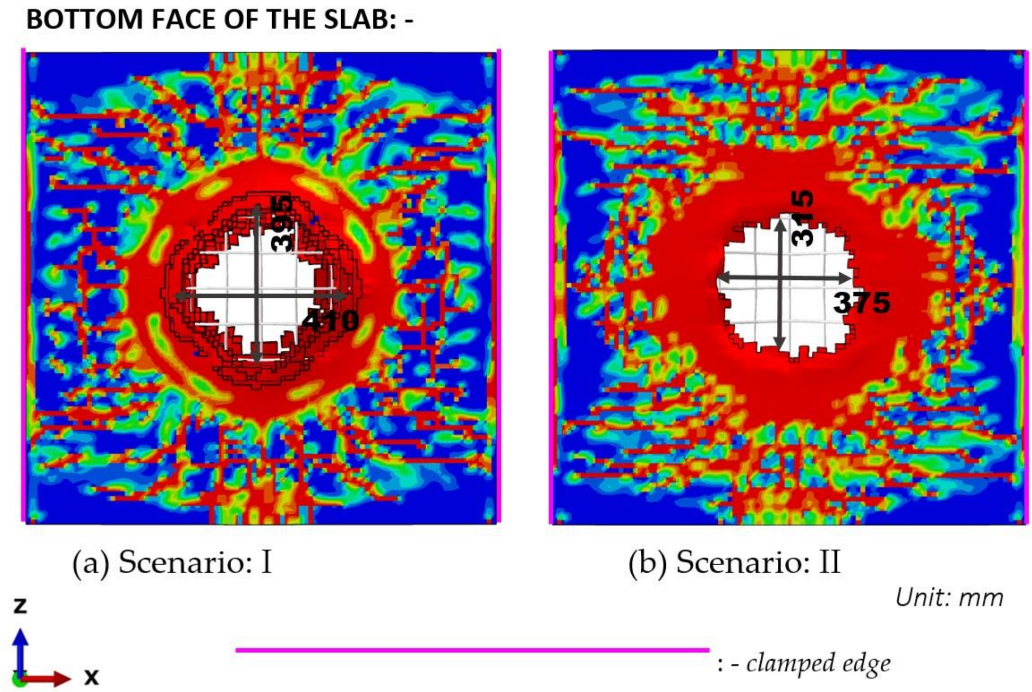

Fig. 7. Damage incurred on the slabs: lower surface.

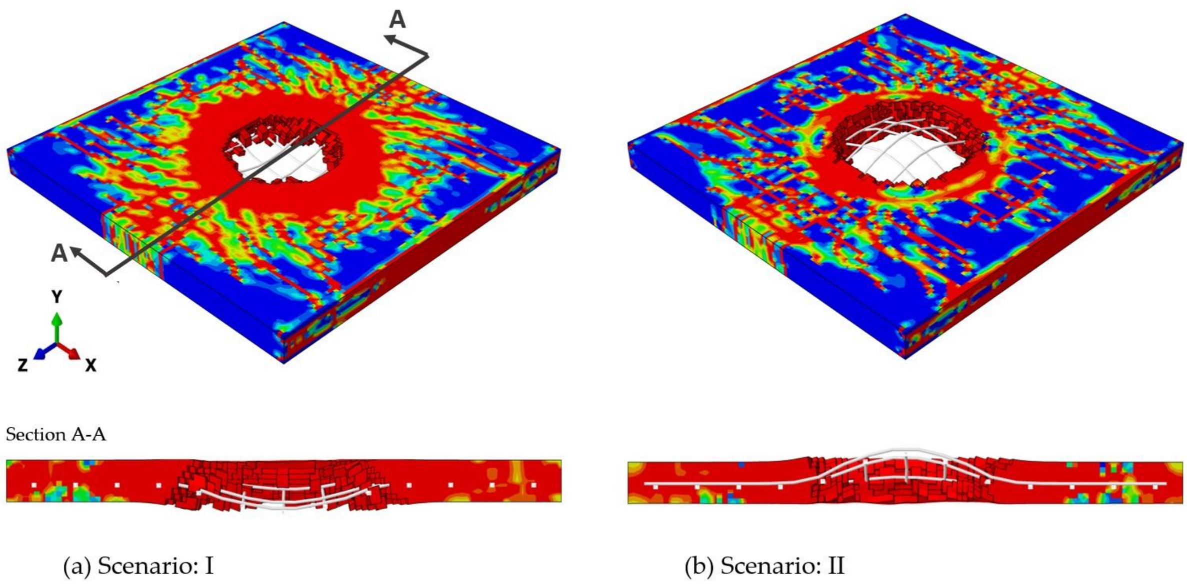

Fig. 8. Slab damage: iso view.

The cumulative plastic deterioration of the slab under Scenario: I amounts to 43.55 joules, whereas under Scenario: II, it escalates to 53.11 joules. It is imperative to note that this degradation is quantified in terms of plastic dissipation energy, denoted in Joules (J). Notably, in Scenario: II, the cracks manifested parallel to the supports exhibit heightened severity in contrast to those observed in Scenario: I. This discrepancy underscores the augmented severity of damage in the slab subjected to central contact detonation at its lower face, commonly known as the tension face.

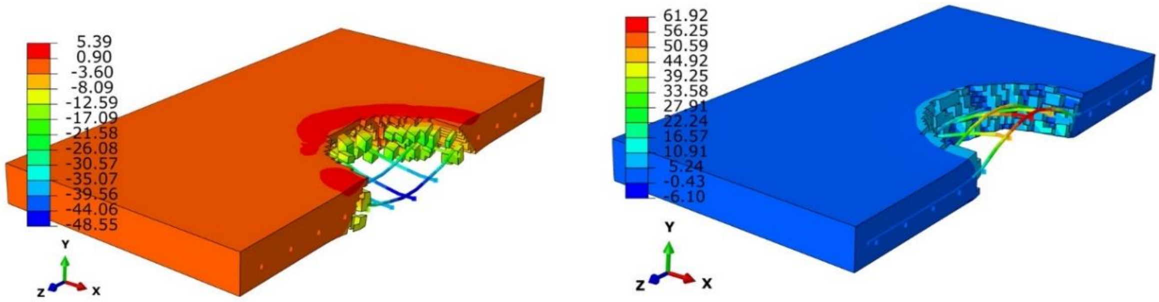

(a) Scenario: I (b) Scenario: II *Unit: mm*

Fig. 9. Deformation of the slabs.

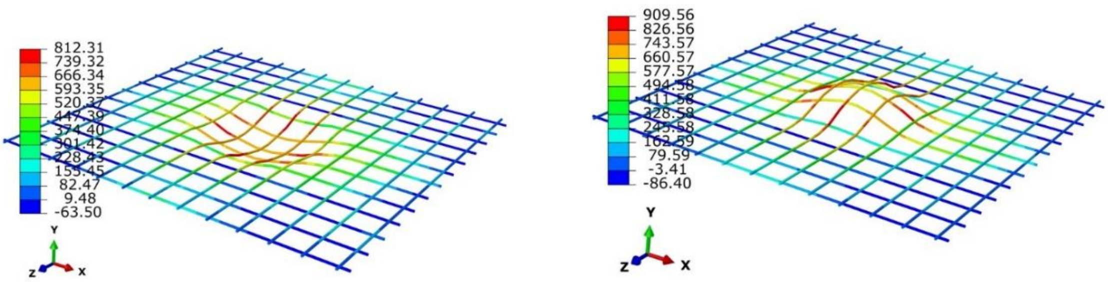

(a) Scenario: I (b) Scenario: II *Unit: MPa*

Fig. 10. Principal stress distribution within the reinforcement of the slabs.

7. Conclusions

This study employs an Integrated Eulerian Lagrangian formulation within the finite element method framework, utilizing the dynamic computational tool Abaqus/Explicit. The aim is to analyze the behavior and effectiveness of a mono-reinforced one-way concrete slab under a central contact explosion. Validation of the numerical model is conducted against publicly available experimental data. Subsequently, the validated model is utilized to investigate the slab's response in two distinct scenarios: In Scenario I, the TNT explosive charge is placed on the compression face, while in Scenario II, it is positioned on the tension face. The conclusions are as delineated below:

- The placement of TNT explosives at the upper surface (compression face) of the slab (Scenario: I) induces significant pulverization, perforation, and deformation, leading to a myriad of damages including cracks, spalling, and punctures. Conversely, in Scenario: II where explosives are positioned at the lower surface (tension face), a reverse phenomenon occurs with increased compression at the lower face and tension at the upper face. This variation in blast placement results in distinct structural responses, with Scenario: II expected to exhibit heightened severity in terms of damage, deformation, and structural failure compared to Scenario: I.
- Scenario: II exhibits significantly higher upward deformation (61.92mm) and tensile stress (909.56 MPa) in reinforcement bars compared to Scenario I (48.55mm and 812.31 MPa respectively), indicating a 1.27-fold increase in deformation and heightened stress intensity.
- The plastic deterioration is notably greater in Scenario: II, with 53.11 joules dissipated, compared to 43.55 joules in Scenario I. Additionally, Scenario: II demonstrates more severe cracking patterns, particularly parallel to supports, emphasizing the intensified damage inflicted on the slab's tension face.

It is noteworthy to underscore that the placement of a contact explosive charge is not confined solely to the upper surface of a slab or roof, such as in the configuration of a suitcase bomb or similar device. Indeed, this research elucidates that the deployment of a contact explosive beneath the lower surface of the slab is a plausible scenario, which warrants consideration.

References

1. S.M. Anas, M. Alam, M. Umair, Air-blast and ground shockwave parameters, shallow underground blasting, on the ground and buried shallow underground blast-resistant shelters: A review. *International Journal of Protective Structures, SAGE* **13**(1), 99-139 (2021)
2. S.M. Anas, M. Alam, M. Umair, Experimental and Numerical Investigations on Performance of Reinforced Concrete Slabs under Explosive-induced Air-blast Loading: A state-of-the-art review. *Structures, Elsevier* **31**, 428-461 (2021)
3. H. Hao, Y. Hao, J. Li, W. Chen, Review of the current practices in blast-resistant analysis and design of concrete structures. *Advances in Structural Engineering, SAGE* **19**(8), 1193-1223 (2016).
4. C. Zhao, X. Lu, Q. Wang, A. Gautam, J. Wang, L.Y. Mo, Experimental and numerical investigation of steel-concrete (SC) slabs under contact blast loading, *Engineering Structures, Elsevier,* **196**, (2019).
5. M.G. Alonso, A.D. Cendon, F. Galvez, B. Erice, S.V. Galvez, Blast response analysis of reinforced concrete slabs: experimental procedure and numerical simulation. *Journal of Applied Mechanics* **78**(5), 1-12 (2011)
6. R. Castedo, P. Segarra, A. Alanon, M.L. Lopez, P.A. Santos, A.J. Sanchidrian, Air blast resistance of full-scale slabs with different compositions: numerical modeling and field validation. *International Journal of Impact Engineering* **86**, 145-156 (2015)
7. Z. Guo, Z. Xu, C. Chen, B. Zhang, E.D. Lehman, S. Cao, Behavior of GFRP retrofitted reinforced concrete slabs subjected to conventional explosive blast. *Materials and Structures, Springer* **50**(236), 1-15 (2017)
8. J. Li, H. Hao, Numerical study of concrete spall damage due to blast loads. *International Journal of Impact Engineering, Elsevier* **68**, 41-55 (2014)
9. J. Li, C. Wu, H. Hao, Y. Su et al., Investigation of ultra-high-performance concrete under static and blast loads, *International Journal of Protective Structures* **6**(2), 217-235 (2015)
10. J. Li, C. Wu, H. Hao, Investigation of ultra-high performance concrete slab and normal strength concrete slab under contact explosion. *Engineering Structures, Elsevier* **102,** 395-408 (2015)
11. A. Schenker, I. Anteby, E. Gal, Y. Kivity, E. Nizri, O. Sadot, R. Michaelis, O. Levintant, G. Ben-Dor, Full-scale field tests of concrete slabs subjected to blast loads. International Journal of Impact Engineering, Elsevier **35**(3), 184-198 (2008)
12. F.P. Silva, B. Lu, "Improving the blast resistance capacity of RC slabs with innovative composite materials. *Composites Part B: Engineering, Elsevier* **38**(5-6), 523-534 (2007)
13. C. Zhao, Q. Wang, X. Lu, J. Wang, Numerical study on dynamic behaviors of NRC slabs in containment dome subjected to close-in blast loading. *Thin-Walled Structures* **135**, 269-284 (2019)
14. Y. Qu, X. Li, X. Kong, W. Zhang, X. Wang, Numerical simulation on dynamic behavior of reinforced concrete beam with initial cracks subjected to air blast loading. *Engineering Structures* **128**, 96–110 (2016)
15. W. Wang, D. Zhang, F. Lu, S.C. Wang, F. Tang, Experimental study on scaling the explosion resistance of a one-way square reinforced concrete slab under a close-in blast loading. *International Journal of Impact Engineering* **49**, 158–64 (2012)
16. D. Zhang, S. Yao, F. Lu, X. Chen, G. Lin, W. Wang et al., Experimental study on scaling of RC beams under close-in blast loading. *Engineering Failure Analysis* **33**, 497–504 (2013)
17. S. Yao, D. Zhang, X. Chen, F. Lu, W. Wang, Experimental and numerical study on the dynamic response of RC slabs under blast loading. *Engineering Failure Analysis, Elsevier* **66**, 120-129 (2016)
18. F.C. Zhao, J.Y. Chen, Y. Wang, S.J. Lu, Damage mechanism and response of reinforced concrete containment structure under internal blast loading. *Theoretical Applied Fracture Mechanics* **61**, 12–20 (2012)
19. S.M. Anas, R.N. Al-Dala'ien, R. Tahzeeb, M. Alam, Non-linear Dynamic Response of Slab with Different Boundary Conditions Subjected to Contact Explosion. *Lecture Notes in Civil Engineering* **474**, (2024)
20. S. M. Anas, M. Alam, M. Asatov, U. Djuraev, Effect of Obliquely Directed Brick TNT Explosive on Slab Response under Contact Explosion. *E3S Web Conf.* **497** (2024)
21. CAE Abaqus, Damage Plasticity, explicit platform, material library, interactions, constraints, boundary conditions, loads, post-processing, Help & Learning manual, *ABAQUS DS-SIMULIA* (2020).
22. S. M. Anas, M. Shariq, M. Alam, M. Umair, Evaluation of Critical Damage Location of Contact Blast on Conventionally Reinforced One-way Square Concrete Slab applying CEL-FEM Blast Modeling Technique. *International Journal of Protective Structures, SAGE* **13**(4), 672-715 (2022)
23. R. N. Al-Dala'ien, A. Syamsir, F. Usman, M.J. Abdullah, The effect of the W-shape stirrups shear reinforcement on the dynamic behavior of RC flat solid slab subjected to the low-velocity impact loading. *Results in Engineering* **19**, 101353 (2023).
24. R. N. Al-Dala'ien, A. Syamsir, M. S. Abu Bakar, F. Usman, M. J. Abdullah, Failure Modes Behavior of Different Strengthening Types of RC Slabs Subjected to Low-Velocity Impact Loading: A Review. *Journal of Composites Science* **7**(6), 246 (2023)

25. R. N. Al-Dala'ien, A. Syamsir, M. S. Abu Bakar, F. Usman, M. J. Abdullah, The effect of continuous rectangular spiral shear reinforcement on the dynamic behavior of RC solid slab subjected to low-velocity impact loading. *Results in Engineering* **21**, 101942 (2024)